Int. J. Electrochem. Sci., 16 **(2021)** Article ID: 210367, doi; 10.20964/2021.03.58

International Journal of
ELECTROCHEMICAL
SCIENCE
www.electrochemsci.org

Corrosion Behavior of Steel Rebar in Cemented Tailings Backfill in Brine

Wensheng Lyu[1], *Liyi Zhu*[1,*], *Peng Yang*[1,2], *Zhixiang Lin*[3], *Zhikai Wang*[4], *Kun Wang*[5]

[1] School of Civil and Resource Engineering, University of Science and Technology Beijing, Beijing 100083, China
[2] Beijing Key Laboratory of Information Service Engineering, Beijing Union University, Beijing 100101, China
[3] 263 Brigade of Jiangxi Nuclear Industry Geology Bureau, Jian 343100, China
[4] China Enfi Engineering Corporation, Beijing 100038, China
[5] College of Energy and Mining Engineering, Shandong University of Science and Technology, Qingdao 266590, China
[*]E-mail: zly0095@126.com

Received: 26 November 2020 / *Accepted:* 13 January 2021 / *Published:* 31 January 2021

In order to investigate the effect of brine on the corrosion process of rebar in the backfill of the mine and the strength of the backfill, four kinds of anti-corrosion measures, such as passivation, water-soluble rust inhibitor, epoxy resin, epoxy resin and water-soluble rust inhibitor combination, were selected. The corrosion behavior of rebar in the backfill mixed with brine was studied by electrochemical test, and compared with that of backfill mixed with deionized water. At the same time, the influence of brine on the early, middle and long-term strength of filling sample was analyzed by uniaxial compression test and XRD test. The results showed that the brine had a significant corrosion effect on the rebar in the backfill, and the combination of epoxy resin and water-soluble rust inhibitor had the best effect among the four anti-corrosion measures. The effect of brine increased the content of ettringite, which in turn increased the early strength of the test sample of the backfill, but the rebar in the test sample was constantly corroded, and the corrosion products were not conducive to the long-term strength.

Keywords: Brine; Backfill; Rebar; Corrosion behavior; Electrochemical test; Strength

1. INTRODUCTION

With the rapid development of economy, the mining intensity of mineral resources is increasing, and the mineral resources in the shallow land are basically exhausted. Most of the mines in the world are advancing to deep mining one after another[1-3], and even many coastal mines are carrying out seabed mining[4, 5]. In addition, with the requirements of maximum recovery of resources and green sustainable development in mining, backfilling mining has become the preferred mining method in

current mining operations[6, 7]. In the coastal and seabed filling mining, the water used in backfilling is often of high brine concentration, which causes serious corrosion to the rebar in the backfill. For example, some deposits are buried in the sea floor, and the joints and structures are often developed in the mining area. During the mining process, the high concentration mineralized bedrock brine remaining in the fractures flows out and flows into the bottom sump, which is diluted and then used as filling water. In the filling process, the artificial roof of the backfill is cemented classified tailings, cement and rebar in a certain proportion, which can be regarded as a special reinforced concrete material. As we all know, reinforced concrete is a widely used and economical building material, which has been widely used in civil infrastructure[8]. At present, many researchers have studied the corrosion behavior of rebar in different concrete environments. Shi et al.[9] studied the influence of different simulated concrete pore solutions on rebar passivation through electrochemical methods such as linear polarization, electrochemical impedance spectroscopy, cyclic polarization and Mott Schottky curve, and concluded that the higher the pH of the simulation solution, the faster the passivation. Sola et al. [10]studied the migration of corrosion products of rebar in concrete by using accelerated corrosion test and numerical simulation, and established a three-dimensional mechanical model of coupling between chemical and moisture heat for corrosion process of cracked concrete. McCarthy et al. [11]studied the influence of cement components, carbonation and chloride ions on the corrosion of rebar in concrete containing wet fly ash. In addition, according to the literatures[12, 13] on corrosion protection of rebar in concrete, it is found that coating is a feasible way to solve the corrosion of rebar.

In general, the backfill can maintain good stability and sufficient strength. However, in salt bittern environment, some ions in brine will react with the hydration products of cement, weaken the hydration reaction, and corrode the cemented products that have been formed, resulting in gel failure. In this case, it can cause corrosion damage of the backfill, reduce the strength of the backfill and make it fail and collapse. More dangerous is the free chloride ion, which will cause electrochemical corrosion of rebar in the backfill, accelerate the corrosion rate of rebar, reduce the mechanical properties of rebar, shorten its service life and even failure. However, at present, most of the researches focus on the corrosion and protection of rebar in concrete in conventional environment, and there are few reports on the corrosion and protection of rebar in coastal or seabed mining fillings.

In this paper, the tailings and cement are mixed with brine, and then rebar are added to form a cemented test sample, which is cured in the brine. Explore the electrochemical characteristics of the self-corrosion potential, polarization curve, impedance spectrum and other anti-corrosion measures of rebar under passivation, water-soluble rust inhibitor, epoxy resin, combination of water-soluble rust inhibitor and epoxy resin. Uniaxial compressive strength test and XRD analysis were used to study the effect of brine on the early, medium and long-term strength of the backfill embedded with rebar, and the influence mechanism was analyzed.

2. EXPERIMENTAL

2.1 Material and solution

Type HPB235 rebar was used in the experiments. Its chemical composition is shown in Table 1. The specimens for electrochemical measurements were welded to a copper wire, and epoxy resin was

coated on the weld[14]. The working surface was abraded with SiC papers of grit size from 400# to 1200# and cleaned with alcohol and distilled water. The corrosion solution in the test was high concentration brine for filling of Sanshandao gold mine, Shandong Province, China. The mass concentration of Na^+, K^+, Ca^{2+}, Mg^{2+}, Cl^-, SO_4^{2-}, CO_3^{2-} and HCO_3^- were analyzed. The analysis results are shown in Table 2. Water-soluble rust inhibitor obtained from Beijing kamabela Technology Co., Ltd, China. The main component was compound amino alcohol, which was prepared by the reaction of small molecule amine and epoxy derivative, and finally diluted into an aqueous solution. The effective content of compound amino alcohol in the aqueous solution was 17%, the density was 1.03 g/cm^3, and the pH was 9.6. Epoxy resin (E-44) purchased from Nantong star synthetic materials Co., Ltd, Jiangsu, China.

Table 1. Chemical composition of steel rebar (wt%)

C	Si	Mn	S	P	Fe
0.220	0.300	0.650	0.050	0.045	Bal.

Table 2. Ion concentration composition of brine

Composition	Na^+	K^+	Ca^{2+}	Mg^{2+}	Cl^-	SO_4^{2-}	HCO_3^-	CO_3^{2-}
Content (mg/L)	14118	263	4275	1440	31392	1981	62.8	Bal.

2.2 Sample preparation of filling sample

In order to be similar to the actual production environment of mine, a corrosion test of the rebar in the tailings cemented test sample was designed to simulate the corrosion of the rebar in the backfill by brine. In the test, the tailings and gelling agent (portland cement) used for cemented the test sample of the backfill were all from Sanshandao Gold Mine. The particle size distribution of the two materials is shown in Fig. 1. The density and specific surface area of gelling agent are 3.1 g/cm^3 and 2.382 m^2/cm^3, respectively. According to the test scheme, the cement/sand(C/S) ratio is 1:6, the slurry concentration is 70%, and the tailings backfill test sample was cemented. The size of the test sample is 40 mm × 40 mm × 160 mm. In order to ensure that the rebar was always kept in the center of the test sample and sufficient thickness of protective layer, suspending rebar and combining with secondary cemented is adopted, as shown in Fig. 3 and 4.

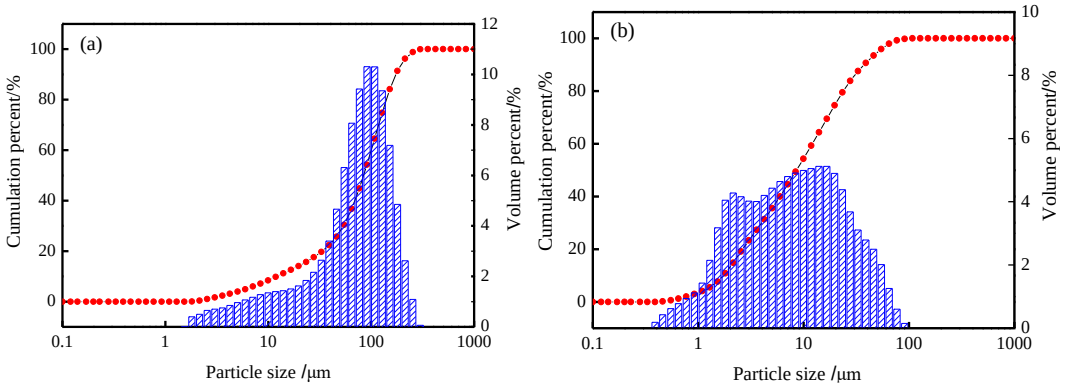

Figure 1. Particle size distribution of materials: (a)classified tailings (b) gelling agent

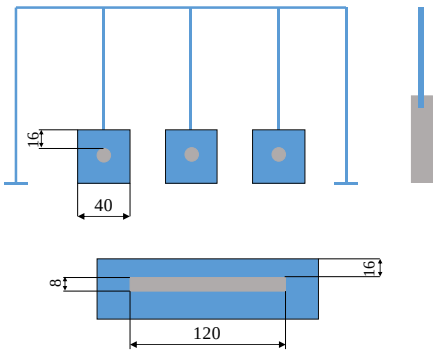

Figure 2. Schematic diagram of rebar size and placement position

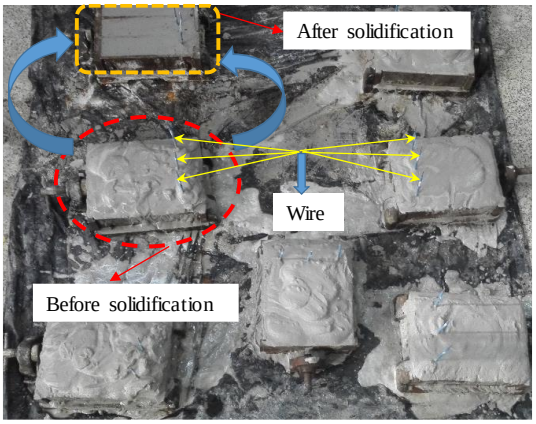

Figure 3. Preparation of backfill test sample

2.3 Experimental program

2.3.1 Corrosion of rebar in tailings cemented test sample by brine filling

There were two kinds of water in the test, one was brine, the other was deionized water. According to the proportioning requirements, the tailings, cement, brine were mixed to prepare slurry,

and the test sample was formed after the rebar was placed. This group of experiments was labeled L_A. The slurry prepared by mixing the tailings, cement and deionized water was used as the control test, which was recorded as Z_A

2.3.2 Experiment on protection of rebar in tailings cemented sample by passivation protection

According to the proportioning requirements, the slurry was prepared after mixing brine, tailings and cement, and the passivated rebar was placed in the slurry to form test samples. The group of tests was marked as L_B. Similarly, the group with deionized water as the test water served as the control group Z_B.

2.3.3 Experiment on protection of rebar in tailings cementation test sample with water-soluble rust inhibitor

Brine, tailing sand and cement were prepared according to the proportioning requirements, and the water-soluble rust inhibitor with the quality of 4.5% cement was added to mix evenly, and the rebar shall be placed to form the test sample. Mark the test as L_C. The control group was treated with deionized water and labeled as Z_C

2.3.4 Experiment of epoxy resin coating on rebar protection in tailings cementation test sample

Brine was used as test water, and the slurry was prepared by mixing it with tailings and cement according to the proportioning requirements. The rebar coated with epoxy resin was placed in the slurry to form a test sample, which was marked as L_D. The experimental water of Z_D in experimental control group was deionized water. In the experimental control group L_E, brine was used as the experimental water, but when the tailings, cement and brine were mixed, a water-soluble rust inhibitor of 4.5% cement mass was added to the slurry.

After the test sample was made, it was allowed to bleed for 24 h, and then it was put into the standard curing box (temperature 20±3 ℃, relative humidity RH ≥ 95%) for 28 d. After the standard box curing, the test sample was placed in brine for half immersion curing. During the curing period, the open circuit potential, polarization curve test and electrical impedance spectrum test of the test sample were carried out continuously, and the data were recorded to understand the corrosion status of rebar.

2.4 Electrochemical measurement

The Versa STATMC electrochemical comprehensive test system(AMETEK Co., America) was used for the electrochemical test, and the three electrode system was used for the test[15]. The working electrode was HPB 235 rebar, the reference electrode was saturated calomel electrode (SCE), the auxiliary electrode was Pt electrode, and the electrolyte was brine. Potentiodynamic polarization test

was carried out after the electrode open circuit potential was stable, and the scanning potential was controlled at - 250 -+ 250 mv (vs.OCP). The scanning rate was 0.5 $mV \cdot s^{-1}$. For electrochemical impedance spectroscopy (EIS) measurements, the frequency ranges from 10^4 Hz to 10^{-2} Hz using an AC amplitude of 10 mV rms was performed at a stable Open-circuit potential (OCP) value. The schematic diagram of electrochemical test and indoor test diagram are shown in Fig. 4 and 5 respectively.

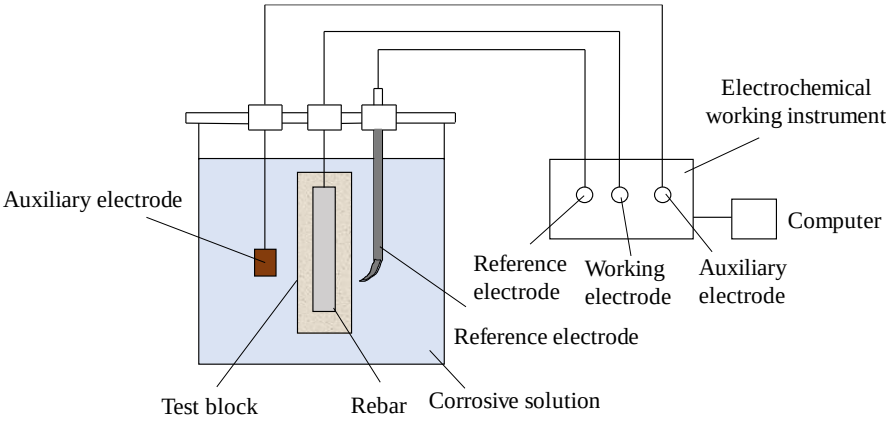

Figure 4. Schematic diagram of electrochemical test

3. RESULTS AND DISCUSSION

3.1 Analysis of self-corrosion potential measurement results

In thermodynamics, self-corrosion potential (E_{corr}) is often used to characterize the trend parameter of corrosion resistance of materials in a specific medium. The larger the negative value of E_{corr} is, the more likely the rebar is to be corroded. Fig. 5 shows the change trend of E_{corr} with curing period in brine environment. It can be seen from Fig. 5 that the E_{corr} of rebar decreased significantly from standard curing to brine curing, and with the increase of curing age in brine, E_{corr} decreased continuously, which indicates that brine had significant corrosion on rebar in backfill. In addition, the E_{corr} of rebar in the test sample prepared with deionized water was higher than that in the sample prepared with brine, but the difference between the two was minor differences. At the later stage of curing, the self-corrosion potential of rebar in the two test samples tends to be the same level. The main reason was that in the curing box (before the brine was half soaked), the test sample with brine had a preliminary corrosion on the rebar, while the deionized water had a weak corrosion effect. However, after the brine was half soaked, the brine seeped into the backfill and corroded the rebar, which made the same effect in the later curing. It can be further found from Fig. 5 that after 4 weeks of standard curing, the E_{corr} of rebar in the backfill with brine was - 635.0 mV (without any protective measures), while under the protective measures such as passivation, adding water-soluble rust inhibitor and coating epoxy resin, E_{corr} was positively moved to - 589.1 mV, - 602.8 mV and - 561 mV respectively. Therefore, it can be preliminarily concluded that the epoxy resin has the most significant anti-corrosion effect on the rebar in the backfill [16,17].

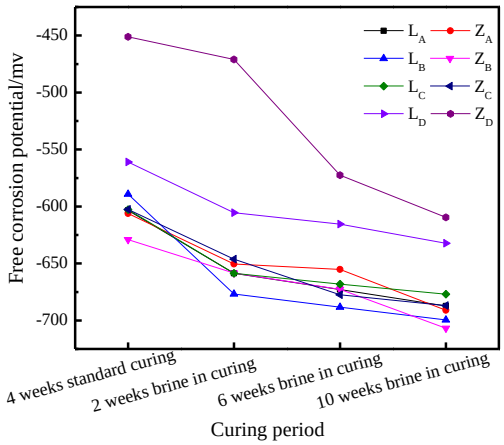

Figure 5. Effect of brine on self corrosion potential of rebar

3.2 Analysis of polarization curve measurement results

Fig. 6 shows the Potentiodynamic polarization curves of rebar with different protective effects in saline water. It can be seen from Fig. 6 that the corrosion current of rebar was reduced under the protective measures such as passivation, water-soluble rust inhibitor and epoxy resin. According to Potentiodynamic polarization curve extrapolation method [18], the current density after immersion curing (L_B) in brine under passivation protection was 199.526 μA/cm^2, that after immersion curing in brine with 4.5% cement mass was 158.489 μA/cm^2, and that of rebar coated with epoxy resin was 0.158 μA/cm^2. Under the protection of epoxy resin and water-soluble rust inhibitor, the current density of (L_E) after soaking and curing in brine was 0.050 μA/cm^2. It can be concluded that the epoxy resin coating can effectively prevent the invasion of corrosive substances and prolong the service life of steel bars [19, 20]. This conclusion is consistent with that obtained by Galliano [21]. The corrosion protection effect of single anti-corrosion measures such as passivation treatment of rebar or adding corrosion inhibitor was not obvious in brine semi immersion environment, so it can be used as additional measures combined with other anti-corrosion measures in practical application.

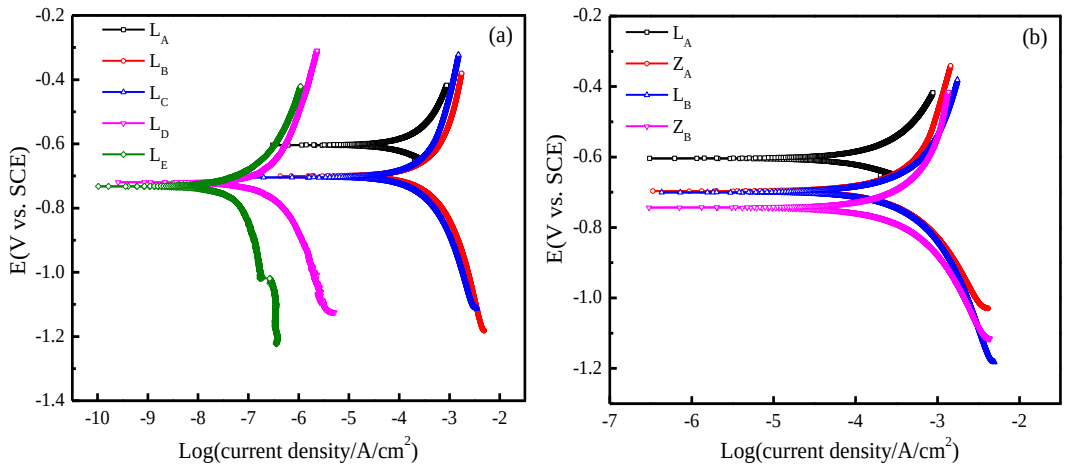

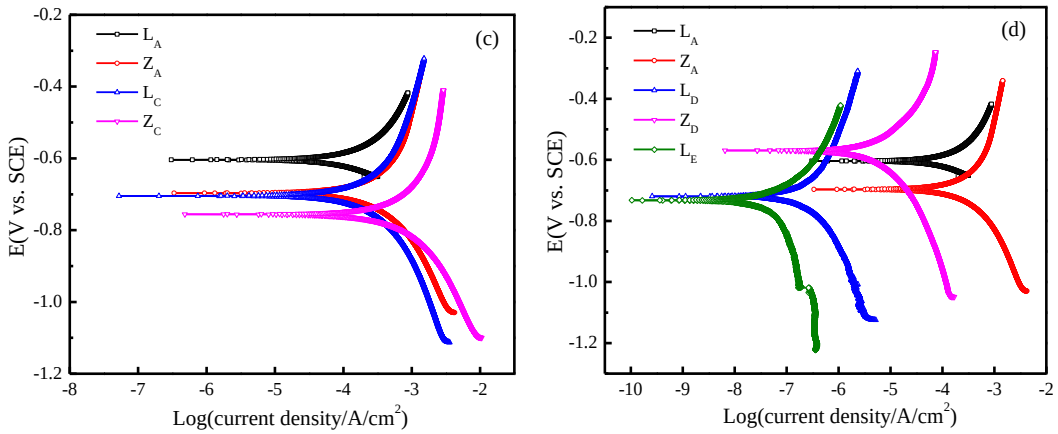

Figure 6. Influence of different protective measures on Tafel polarization curve of rebar: (a)Four anti-corrosion measures (b) Passivation (c) Water-soluble rust inhibitor (d) Epoxy resin

3.3 Analysis of EIS measurement results

Fig. 7 shows the Nyquist diagram of EIS curve obtained after rebar was passivated and soaked in brine for 4 weeks. Fig. 8 shows the Nyquist diagram of EIS curve of rebar with different curing periods under the conditions of epoxy resin protection and combination protection of epoxy resin and water-soluble rust inhibitor. It can be seen from Fig. 7 that after the rebar was soaked in brine, there was no obvious large-diameter capacitive arc in the low-frequency region for both the steel bars with passivation protection and those without protection, which indicated that the corrosion protection effect of passivation on steel bars in brine was not significant [22-25]. It can be seen from Fig. 8 that the capacitance arc diameter of the rebar in the low frequency region was larger under the epoxy resin coating, which indicated that the epoxy resin effectively played an anti-corrosion role in the filling and cementing test sample. Especially under the protection of epoxy resin and water-soluble rust inhibitor, there were two obvious large diameter of capacitive arc, which further proved that the combination of epoxy resin and water-soluble rust inhibitor has the best anti-corrosion effect on rebar.

The effective impedance of corrosion system was simulated and analyzed by ZsimpWin software according to the equivalent circuit diagram in Fig. 9. The fitting results are shown in Table 3. In Fig. 9, R_S was the resistance of corrosion solution, R_1 was the resistance of protective layer, Q_1 was the capacitance of protective layer, R_2 was the charge transfer resistance of rebar interface, and Q_2 was the electric double layer capacitance of rebar interface. It can be seen from Table 3 that the double-layer capacitance of rebar interface was small under epoxy resin coating. After 10 weeks of curing, the double-layer capacitance of rebar coated with epoxy resin in brine environment was 8.712×10^{-13} $\Omega^{-1}\cdot cm^{-2}\cdot s^{-n}$, which indicated that epoxy resin has strong anti-corrosion effect.

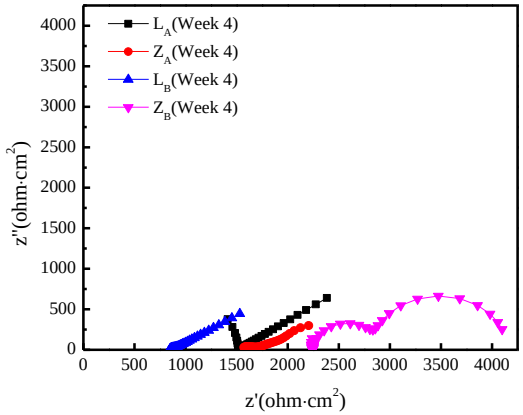

Figure 7. Influence of passivation on EIS curve of rebar

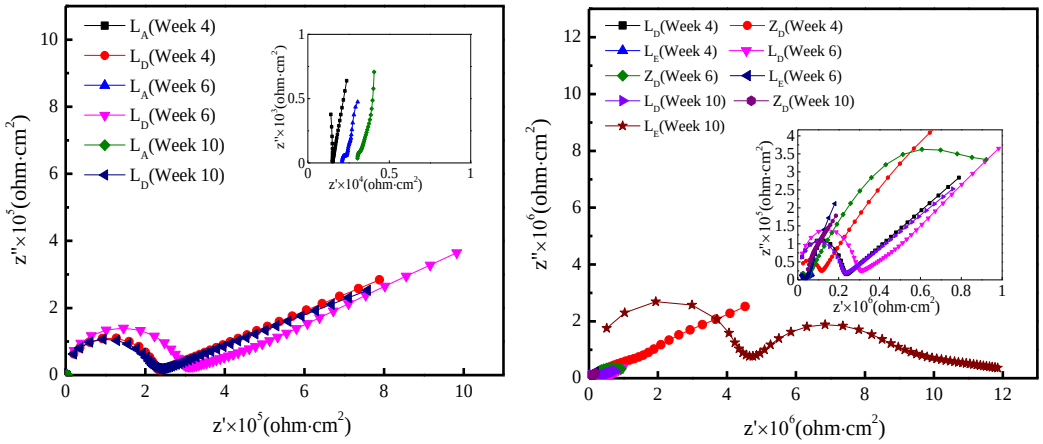

Figure 8. Influence of epoxy coating on EIS curve of rebar

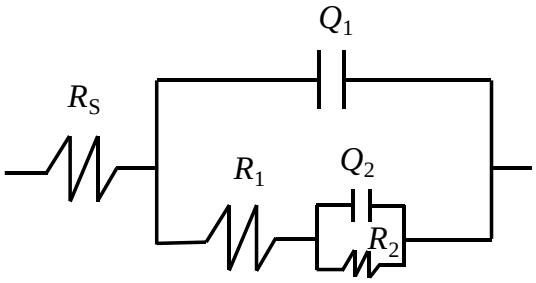

Figure 9. Equivalent circuit models used to fit EIS data of rebars

Table 3. EIS parameters obtained from data fitting for rebar at different immersion times.

Test group	Q_1 ($\Omega^{-1}\cdot cm^{-2}\cdot s^{-n}$)	R_1 ($\Omega\cdot cm^2$)	Q_2 ($\Omega^{-1}\cdot cm^{-2}\cdot s^{-n}$)	R_2 ($\Omega\cdot cm^2$)
L_{A-4}	5.207×10^{-11}	7.998×10^{3}	3.780×10^{-5}	1.333×10^{4}
Z_{A-4}	2.951×10^{-7}	6.841×10^{2}	1.050×10^{-4}	1.026×10^{4}
L_{B-4}	7.618×10^{-6}	1.007×10^{3}	2.997×10^{-5}	5.839×10^{3}
Z_{B-4}	1.376×10^{-5}	4.332×10^{3}	1.158×10^{-4}	6.599×10^{3}

L_{D-4}	2.868×10^{-12}	1.353×10^{6}	6.144×10^{-8}	6.061×10^{6}
L_{E-4}	6.974×10^{-12}	1.703×10^{5}	3.938×10^{-1}	4.713×10^{5}
L_{A-6}	7.769×10^{-8}	8.319×10^{2}	7.824×10^{-5}	2.202×10^{4}
L_{D-6}	1.538×10^{-7}	2.969×10^{1}	1.709×10^{7}	1.467×10^{-2}
Z_{D-6}	2.258×10^{-8}	6.884×10^{6}	6.201×10^{-6}	3.838×10^{-1}
L_{E-6}	5.995×10^{-11}	1.855×10^{5}	2.649×10^{-7}	1.465×10^{16}
L_{A-10}	5.132×10^{-9}	9.786×10^{2}	7.242×10^{-6}	1.803×10^{4}
L_{D-10}	2.148×10^{-7}	$2.907\times10^{-}$	8.712×10^{-13}	1.761×10^{15}
Z_{D-10}	2.837×10^{-9}	1.274×10^{6}	5.994×10^{-8}	2.165×10^{16}
L_{E-10}	2.039×10^{-10}	6.832×10^{7}	1.644×10^{-15}	1.913×10^{18}

The subscripts 4, 6, and 10 for the test group indicate the number of weeks of immersion in brine water, respectively.

3.4 Effect of rebar corrosion in brine on the strength of cemented tailings backfill

In order to explore the influence of brine corrosion on the early and medium long-term strength of the backfill, the 70 wt% slurry was prepared by adding brine, and the evenly stirred slurry was made a test sample with the size of 7.07 cm × 7.07 cm × 7.07 cm. According to the same parameters, deionized water was added to make the test sample with the same size as the control group. After curing with 20 ℃ for 24 h, the specimen was demoulded, and then put into the curing box for standard curing (20 ± 0.5 ℃, relative humidity of 95%), curing for 3 d, 7 d, 14 d, 28 d, 60 d, 90 d and 120 d. The compressive strength of the test sample was tested during the curing period, and the results are shown in Table 5. It can be found from Table 5 that the uniaxial compressive strength of the filling sample made of brine mixture with C/S ratio of 1:6 increases from 1.461 MPa in 3 d curing period to 4.373 MPa (28 d curing period). When the C/S ratio is 1:10, the filling sample increases from 0.607 MPa to 1.938 MPa. Compared with the sample with deionized water, the uniaxial compressive strength of the sample increased by 80.92% (28 d, 1:6) and 19.56% (28 d, 1:10), respectively. However, after 60 days of curing, the compressive strength of the test sample mixed with deionized water was higher than that of the test sample mixed with brine. The lower the C/S ratio was, the smaller the difference of compressive strength between them was.

In order to explore the mechanism of the influence of brine on the strength of the filler test sample, XRD pattern analysis was performed on the cemented test sample mixed with deionized water and the cemented test sample mixed with brine. The results are shown in Fig. 10. It can be seen from Fig. 10 that the diffraction peaks of C-S-H gel and portlandite in the brine cemented test sample were obviously larger in number and higher in intensity. Due to the presence of large amount of SO_4^{2-} in brine, it can contribute to ettringite production. Yu et al. [26] found that SO_4^{2-} can produce corrosion on concrete. Although ettringite affects the final strength of backfill[18, 27], the positive effect of C-S-H gel and calcium hydroxide on the early strength was more obvious. According to the above experimental results, brine filling was helpful to improve the early strength of the backfill.

The later strength of the test sample with embedded rebar was tested, and the results are shown in Fig. 11. It can be seen from Fig. 11 that the compressive strength of the test sample mixed with deionized water was higher than that of the test sample mixed with brine. When the C/S ratio is 1:6 and

the curing age was 120 d, the compressive strength of the two test samples was less than that of the test samples mixed with brine in the medium and long term. Because the test sample with embedded rebar was cured by half soaking in brine, the corrosion products of rebar are enriched in the internal part of the test sample, which affects the hydration and gelation during the curing period of the test sample; in addition, the occurrence of dry and wet circulation was conducive to the formation of salt crystallization, which aggravates the corrosion of the test sample by brine.

Fig. 12 shows the color change of the test sample with or without epoxy resin coating after adding with brine. The rebar without epoxy resin coating was seriously corroded by brine, and the main corrosion behaviors were pitting corrosion and local corrosion. There were a lot of deep pitting pits on the surface of rebar, and the cross-sectional area of rebar is reduced. The existence of pitting pits will accelerate the corrosion rate of rebar, resulting in uneven corrosion of rebar, which will seriously affect the mechanical properties of rebar. On the contrary, the surface of the rebar coated with epoxy resin still showed metallic luster, and the color was mainly black and silver white, which indicated that there was no corrosion or slight corrosion in these parts. Only yellowish brown rust spots were found locally, and no obvious corrosion marks were found, which showed slight corrosion. These corrosion traces mainly concentrated in the places with poor quality of epoxy resin coating. Compared with the color change inside the test sample and the surface characteristics and color changes of the rebar corrosion, it showed that the brine will cause serious corrosion to the rebar in the test sample. It was further verified that the epoxy resin coating can effectively protect the rebar and delay the corrosion of rebar by brine[28-30].

Table 4. Medium and long term uniaxial compressive strength of cemented tailing test sample

Cement-sand ratio	Mixing water	Compressive strength of different curing ages/MPa						
		3 d	7 d	14 d	28 d	60 d	90 d	120 d
1:6	Brine	1.461	2.406	3.344	4.373	6.936	8.632	9.926
	Deionized water	0.897	1.439	1.831	2.417	7.461	9.169	10.636
1:10	Brine	0.607	1.247	1.524	1.938	2.642	3.324	4.187
	Deionized water	0.483	0.991	1.268	1.621	2.718	3.589	4.538

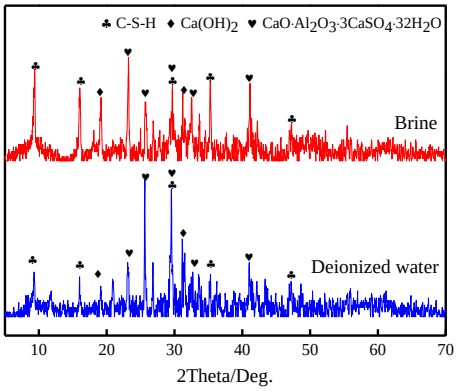

Figure 10. XRD diffraction pattern

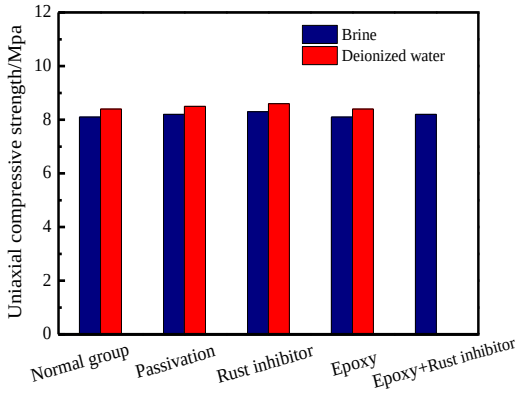

Figure 11. Uniaxial compressive strength of embedded reinforced backfill with different anti-corrosion conditions

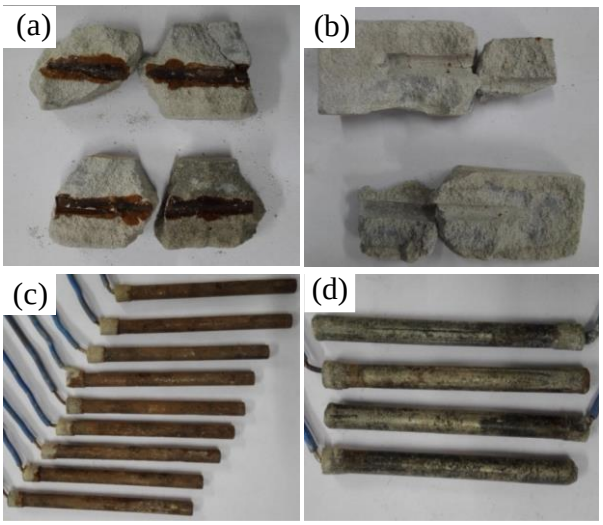

Figure 12. Color change of test sample and rebar coated with and without epoxy resin: (a) Test sample without epoxy coating (b) Epoxy coated test sample (c) Rebar without epoxy coating (d) Rebar with epoxy coating

4. CONCLUSIONS

Brine had a significant corrosive effect on rebar. Epoxy resin can effectively protect the corrosion of rebar from brine. After a certain curing period, the E_{corr} increased from -635.0 mV (without anti-corrosion measures) to -561 mV, and the current density was 0.158 μA/cm^2. Epoxy resin combined with water-soluble rust inhibitor (4.5% of the mass of cement) had a better anti-corrosion effect, and the current density was as low as 0.050 μA/cm^2. Passivation and the addition of water-soluble rust inhibitors cannot effectively prevent the corrosion of rebar in the backfill by brine.

Brine had certain influence on the strength of filling test sample. In the early stage of cementation curing, brine can improve the compressive strength of cemented test sample. When the curing period was 28 days and the C/S ratio was 1:6 and 1:10, the strength of the test sample mixed with deionized water was increased by 80.92% (28 days, 1:6) and 19.56% (28 days, 1:10), respectively. In the later

stage of backfill curing, the strength of deionized water mixing test sample was greater than that of brine mixing test sample. The lower the C/S ratio was, the smaller the difference of compressive strength between them was.

XRD analysis showed that the diffraction peaks of C-S-H gel and calcium hydroxide were obviously larger and the intensity was higher. A large amount of SO_4^{2-} in brine was beneficial to ettringite production, which promotes gel of C-S-H gel and calcium hydroxide and improves early strength. However, in the later stage of curing, the ultimate compressive strength of the brine mixed cementation test sample was not as high as that of the deionized water mixed test sample.

ACKNOWLEDGMENTS
This research was supported by the National Key Research and Development Project of China (2017YFC0804604), the National Science Foundation of China (51774045).

References

1. M. Li, X. P. Zhang, S. J. Mao and Q. S. Liu, *Procedia Earth Planet. Sci.*, 1 (2009) 377.
2. P.G. Ranjith, J. Zhao, M. Ju, R.V.S. De Silva, T.D. Rathnaweera and A.K.M.S. Bandara, *Eng.*, 3 (2017) 546.
3. Q. Wang, Z. Jiang, B. Jiang, H. Gao, Y. Huang and P. Zhang, *Int. J. Rock Mech. Min.*, 128 (2020) 104264.
4. A.S. Levine, L. Richmond and D. Lopez-Carr, *Appl. Geogr.*, 59 (2015) 56.
5. K. Peng, X. B. Li, C. C. Wan, S. Q. Peng and G. Y. Zhao, *Trans. Nonferrous Met. Soc. China*, 22 (2012) 740.
6. Z. Yang, S. Zhai, Q. Gao and M. Li, *J. Rock Mech. Geotech. Eng.*, 7 (2015) 87.
7. L. Zhu, W. Lyu, P. Yang and Z. Wang, *Ultrasoni. Sonochem.* 66 (2020) 104984.
8. Z. Ai, J. Jiang, W. Sun, D. Song, H. Ma, J. Zhang and D. Wang, *Appl. Surf. Sci.* 389 (2016) 1126.
9. J.J. Shi, W. Sun and G.Q. Geng, *J. Build. Mater.*, 14 (2011) 452-458.
10. E. Sola, J. Ožbolt, G. Balabanić and Z.M. Mir, *Cem. Concr. Res.*, 120 (2019) 119.
11. M.J. McCarthy, P.A.J. Tittle and R.K. Dhir, *Cem. Concr. Compos.*, 102 (2019) 71.
12. S. Pour-Ali, C. Dehghanian and A. Kosari, *Corros. Sci.*, 90 (2015) 239.
13. A. Fihri, E. Bovero, A. Al-Shahrani, A. Al-Ghamdi and G. Alabedi, *Colloids Surf., A*, 520 (2017) 378.
14. J. Li, *Int. J. Electrochem. Sci.*, 15 (2020) 7136.
15. S.S. Xin, M.C. Li, *Corros. Sci.*, 81 (2014) 96.
16. G. D. Li, Y. Wang and Z. Q. Cao, *J. Chem. Eng.*, 63 (2012) 560.
17. Y. Wang, Z. B. Cao, W. W. Sun and F. J. Zhang, *Compr. Corros. Control*, (2009) 23.
18. H. Nguyen, E. Adesanya, K. Ohenoja, L. Kriskova, Y. Pontikes, P. Kinnunen and M. Illikainen, *Constr. Build. Mater.*, 197 (2019) 143.
19. Z. Li, W. Yang, Q. Yu, Y. Wu, D. Wang, J. Liang and F. Zhou, *Langmuir*, 35 (2019) 1134.
20. M.D. Yu, C.Q. Fan, S.K. Han, F. Ge, Z.Y. Cui, Q.Y. Lu and X. Wang, *Prog. Org. Coat*., 147 (2020) 105867.
21. F. Galliano, D. Landolt, *Prog. Org. Coat.*, 44 (2002) 217.
22. A. Amirudin, D. Thieny, *Prog. Org. Coat.*, 26 (1995) 1.
23. S. Taylor, E. Gileadi, *Corrossion*, 51 (1995) 664.
24. E. Warburg, *Ann. Phys.*, 303 (1899) 493.
25. E. B. Caldona, D. O. Wipf and D. W. Smith Jr, *Prog. Org. Coat.*, 151 (2021) 106045.

26. H.F. Yu, J.C. Wang, W. Qu, L.H.Yan and Z.Y. Wei, *J. Chin. Ceram. Soc.*, 31(2003) 434.
27. Q. Fang, *Int. J. Electrochem. Sci.*, (2019) 5042.
28. A.S. El-Dieb, T.A. El-Maaddawy, *J. Build. Eng.*,20 (2018) 72.
29. S. Pour-Ali, C. Dehghanian and A. Kosari, *Corros. Sci.* 90 (2015) 239.
30. A.K. Dermani, E. Kowsari, B.Ramezanzadeh and R. Amini, *J. Ind. Eng. Chem.*, 79 (2019) 353.